

Abstract

This work examines the relationships between Aerosol Optical Depth (AOD) and Particulate Matter (PM_x) parameters, based on long records (2003–2011) of two nearby sites from the AERONET and EMEP networks in the north-central area of Spain. The climatological annual cycle of PM_{10} and $PM_{2.5}$ present a bimodality which might be partly due to desert dust intrusions, a pattern which does not appear in the annual cycle of the AOD. In the case of the AOD, this bimodality is likely to be masked because of the poor sampling of sunphotometer data as compared to PM_x (67 % of days against 90 %), and this fact stresses the necessity of long-term observations. In monthly series, significant interannual variations are observed and most extrema coincide, however the bimodal shape remains relatively stable for PM_x . Significant and consistent trends were found for both datasets likely associated to a decrease of desert dust apportionment until 2009. PM_{10} and AOD daily data are moderately correlated (0.56), a correlation improving for monthly means (0.70). In the case of strong desert dust events day-to-day correlation is not systematic, therefore an extensive analysis on PM_x , fine-PM ratio, AOD and associated Ångström exponent (α) is carried out.

1 Introduction

Airborne ambient particles represent a considerable environmental factor of risk for human health. Indeed, epidemiological studies have extensively shown statistical association between the exposure to particulate air pollution and adverse health effects (Pope III, 2000).

A common reference indicator for particulate air quality is the concentration of particulate matter (PM) at ground level which is given in units of mass per unit volume of air. Since the health impact of particulate air pollution appears to relate most consistently with aerodynamic diameters, which determines the capability of airborne particles to penetrate into the respiratory system, PM concentrations are measured for different

AMTD

7, 5829–5882, 2014

Long-term AOD- PM_x relationships in north-central Spain

Y. S. Bennouna et al.

Title Page

Abstract

Introduction

Conclusions

References

Tables

Figures



Back

Close

Full Screen / Esc

Printer-friendly Version

Interactive Discussion



Long-term AOD-PM_x relationships in north-central Spain

Y. S. Bennouna et al.

Title Page

Abstract

Introduction

Conclusions

References

Tables

Figures



Back

Close

Full Screen / Esc

Printer-friendly Version

Interactive Discussion



To support the regional agencies in their labor of advertisement and AQ Directive compliance duties, a significant effort has been dedicated to the implementation of continuous ground-based in-situ monitoring networks to measure pollution associated to this type of particles/size fraction. Since 1999, all European countries are required to maintain dense PM₁₀ measurements for urban agglomerations of relevant size (EC, 1999, 2008). Besides, other networks such as the European Monitoring and Evaluation Programme (EMEP) network have been established with the objective to study Long-Distance Atmospheric Pollution, thus providing governments with quantitative information on the transport of air pollutants across national boundaries, resulting deposition and concentration levels (Tørseth et al., 2012; Borowiak and De Saeger, 1996). In order to measure only pollution at regional level, the location of EMEP stations must follow a number of requirements: (a) be situated in a rural area, (b) be away from buildings and (c) far enough from industrial sources of pollutants (minimum 40 km), (c) exclude valleys and peaks. The concentrations of PM₁₀ and PM_{2.5} are monitored at many sites of the EMEP network. The data provided by such networks can be used not only to quantify the concentration of these particle fractions, but also to investigate relations between them and to compare their elemental/chemical composition. Despite all these efforts, PM observations are too scarce to resolve the large spatial and temporal variation and thus limit the potential of environmental and health assessment for regulating impacts.

Although detailed measurements can only be achieved in situ, observations of atmospheric aerosols can also be provided by remote sensing techniques. On ground, dense sunphotometer networks such as NASA's AERONET (Aerosol Robotic Network) created in the 1990's provides a continuous database of aerosol remote sensed measurements at more than nearly 400 sites around the globe (Holben et al., 1998). Such networks constitutes a valuable source of information for the establishment of local and regional aerosol characterizations (Holben et al., 2001). A primary parameter provided by remote sensing is the Aerosol Optical Depth (AOD), describing the extinction of the electromagnetic radiation in an atmospheric column attributed to aerosols at a given

wavelength. Hence, this parameter does not directly quantifies the particle loading, as it is obtained by vertically integrating the aerosol concentration weighted with the effective cross-sectional area of those interacting (by scattering and absorption) with the solar radiation at the wavelength of interest (Ramanathan et al., 2001).

Remote sensing from space satellite is the only technology capable to achieve full spatial coverage. Despite the fact that satellite measurements (AOD) are not as accurate as ground-based ones, they represent a cost-effective method to improve the insight in PM spatial distribution and transport patterns, especially in a context of increasing availability of satellite observations (Kokhanovsky et al., 2007). Moreover, aerosol information has started to be retrieved from space a few decades ago over ocean and more recently over land (King et al., 1999).

The availability of PM concentration spatiotemporal maps is crucial for a better understanding of the underlying natural processes and an adequate assessment of PM effects. For this reason, in the recent years there has been a great interest for studies using satellite AOD to monitor and assess air quality. Nevertheless, the AOD is a complex function of the aerosol mass concentration, mass extinction efficiency, relative humidity, and vertical distribution of aerosols, and several authors have investigated the relationships between the latter and PM_x . Some of these studies are based on ground-based AOD measurements (Cachorro and Tanre, 1997; Pelletier et al., 2007; Schaap et al., 2009; Estellés et al., 2012) such as those from AERONET operational network, known to provide well calibrated data and often used for the validation of satellite inversion algorithms. In other works, PM_x data are directly derived from satellite AODs (Kokhanovsky et al., 2009; Koelemeijer et al., 2006; Zhang et al., 2009; Al-Saadi et al., 2005; Vidot et al., 2007). These lead to remote sensing of PM_x using MODIS (Moderate Resolution Imaging Spectroradiometer), MISR (Multi-angle Imaging SpectroRadiometer), MERIS (Medium Resolution Imaging Spectrometer), POLDER (POLarization and Directionality of Earth Reflectances), MSG-SEVIRI (Spinning Enhanced Visible and Infrared Imager) (Liu et al., 2007a, b; Van Donkelaar et al., 2006).

Long-term AOD- PM_x relationships in north-nentral Spain

Y. S. Bennouna et al.

[Title Page](#)[Abstract](#)[Introduction](#)[Conclusions](#)[References](#)[Tables](#)[Figures](#)[Back](#)[Close](#)[Full Screen / Esc](#)[Printer-friendly Version](#)[Interactive Discussion](#)

Long-term AOD-PM_x relationships in north-central Spain

Y. S. Bennouna et al.

Title Page

Abstract

Introduction

Conclusions

References

Tables

Figures



Back

Close

Full Screen / Esc

Printer-friendly Version

Interactive Discussion



A characteristic source of aerosols from natural origin affecting Southern Europe is the dust transported from the Sahara and Sahel deserts. In particular, because of its proximity to the African continent and favorable atmospheric circulation, the area of the Iberian Peninsula is frequently affected by strong episodes of desert dust, when airmasses are advected from the Saharan desert to the Iberian Peninsula under specific synoptic conditions (Artiñano et al., 2001; Rodríguez et al., 2001; Escudero et al., 2005). These dust outbreaks have an important impact on air quality, and some studies have highlighted that most PM₁₀ exceedance observed at regional background stations are associated with those events (Rodríguez et al., 2004; Escudero et al., 2007). Desert dust intrusions are also detected by remote measurement techniques using sunphotometers, based on the AOD and its spectral wavelength dependence with the Ångström exponent parameter (Vergaz, 2001; Vergaz et al., 2005; Lyamani et al., 2005; Cachorro et al., 2006; Toledano et al., 2007b; Cachorro et al., 2008; Toledano et al., 2009). Moreover, owing to the dry climate and scarcity of precipitations the particles accumulate in the atmosphere. Two different types of episodes associated with mineral dust can be linked to the increase of PM concentrations in the central area of the Iberian Peninsula: regional recirculation during summer months and long-range transport processes from spring to autumn time (Coz et al., 2009; Querol et al., 2004).

The objective of this work is to investigate in details the relations between PM_x and AOD data in the northern central area of Spain, through the use of two nearby regional background sites from the EMEP and AERONET networks. Indeed, such relations have been studied in the case of urban atmospheres, but it has not been done for relatively clean atmospheric backgrounds such as it is the case here, and furthermore with the highest levels of PM_x attributed to desert dust intrusions. Besides, it is the first time to our knowledge that such long records are used for this kind of study taking into account 9 years of overlapping data for AOD and PM_x, thus allowing to emphasize on the climatological point of view. Some works investigated the relation PM_x-AOD together with aerosol speciation but in the present study the perspective is different as it uses the Ångström exponent (Alpha) for columnar properties, and the fine-PM ratio

($PM_{2.5}/PM_{10}$) for surface observations. The whole analysis is thus carried out with respect to the climatological aerosol types (e.g. continental, desert, maritime, biomass burning).

The paper starts by briefly introducing the region of study and follows by a description of the different datasets. The results present an analysis of the annual cycle, interannual variability, and trends of PM_x size fractions in relation to those of the AOD. These parameters are examined in parallel with the information of the Ångström exponent and fine-PM ratio in order to address the findings in terms of aerosol size and type. The correlation results between these parameters are also presented both for daily data and monthly averages.

2 Region of study and measurement sites

The locations of the two sites used in this study are presented in Fig. 1. The towns of Peñausende (41.24° N 5.90° W, 985 m a.s.l.) and Palencia (41.99° N, 4.52° W, 750 m a.s.l.) belong to the autonomous community of “Castilla y León” (CyL). This region, situated in the north central part of the Iberian Peninsula lies on the northern plateau of Spain (Castilian Plateau) which has on average an altitude of 700 m, and is crossed by the Duero River forming a narrow valley. The Castilian Plateau is surrounded by mountains of almost uniform height (Pinto et al., 2001). These mountains stand as topographic barriers reducing greatly Atlantic and Mediterranean influences thus leading to the continental climate characterizing this region (Del Rio et al., 2007).

The CyL region extends over a large territory (94 193 km²) with an area of about a fifth of Spain it is the third European region in size. It is the most sparsely populated region of the country with a density around 27 hab km⁻². The biggest metropolitan center of the region is Valladolid (~ 400 000 habitants), the capital of the region. About 50 km to the north-east of Valladolid, Palencia, the capital of its own province, is a small town (~ 100 000 habitants) located in a rural area in the north of CyL. About 200 km to the southwest of Palencia, the little village of Peñausende (~ 500 habitants) belonging

Long-term AOD- PM_x relationships in north-central Spain

Y. S. Bennouna et al.

Title Page

Abstract

Introduction

Conclusions

References

Tables

Figures



Back

Close

Full Screen / Esc

Printer-friendly Version

Interactive Discussion



to the province of Zamora is situated at 26 km of Zamora (~ 65 000 habitants). Both Palencia and Peñausende, are relatively well isolated from big urban and industrial centers, Valladolid being the closest of relevant size, and can therefore be classified as rural regional background stations. Such sites are particularly useful to detect and characterize the impact of desert dust outbreaks (Coz et al., 2009).

3 Datasets

At Peñausende, PM_X measurements have been carried out continuously since 2001 by means of gravimetric methods. The samples are collected on quartz fiber filters using MCV-PM1025 high-volume samplers operating at an average flow rate of $30\text{ m}^3\text{ h}^{-1}$ with $10\mu\text{m}/2.5\mu\text{m}$ cut-off inlets. Sample treatment, analytical procedures and quality assurance are performed according to the details described in the EMEP Manual for Sampling and Chemical Analysis (EMEP, 1996). PM_{10} and $PM_{2.5}$ sampling is carried out on a daily basis (one PM_{10} and one $PM_{2.5}$, 24 h sample/day). Table 1 sums up the number of EMEP PM_X measurements available by year. On average for a year, data are provided about 88 % of the time, with a minimum of 251 days in 2001 when the station started operation, and a maximum of 347 (95 %) in 2007. It can be seen that $PM_{2.5}$ was also continuously measured with PM_{10} , except for the year 2010, for which 12 days are missing. For the full period between 2001–2011, this leads to totals of 3531 and 3519 days for PM_{10} and $PM_{2.5}$ datasets respectively, and to totals of 2969 and 2957 respectively, considering the restricted period 2003–2011 used in this study.

A CIMEL sunphotometer located at the outskirts of Palencia (University Campus, Technical Superior School of Forestry and Agricultural Engineering) and operating in the frame of AERONET-EUROPE (Holben et al., 1998; Goloub et al., 2012), has been providing continuous aerosol measurements from 2003 to 2011 with the exception of 15 months between 2009 and 2010. For climatological and trend analysis (Sects. 4.1 and 4.2), the gaps in Palencia data were completed by values from Autilla, a closeby AERONET site situated a few kilometers from Palencia. In all results of Sect. 4.3

Long-term AOD- PM_X relationships in north-central Spain

Y. S. Bennouna et al.

Title Page

Abstract

Introduction

Conclusions

References

Tables

Figures



Back

Close

Full Screen / Esc

Printer-friendly Version

Interactive Discussion



found that the climatological curves of coinciding days also lead to similar results for all curves (not shown here) and therefore no conclusion can be drawn on that aspect.

However, the bimodality of the climatological annual cycle for the AOD has already been observed at a site of the Iberian Peninsula, located in the south-western coast of Spain, in the area of the Gulf of Cadiz near the city of Huelva (Bennouna et al., 2011). In this area of the Iberian Peninsula, mineral dust events are more frequent and stronger (Toledano et al., 2007b). Figure 3b presents the climatological annual cycle of PM_{10} , $PM_{2.5}$ and AOD (440 nm) based on data from two southern EMEP and AERONET sites, Barcarrota (38.47° N, 6.92° W, 393 m a.s.l., Badajoz) and El Arenosillo (37.10° N, 6.73° W, 0 m a.s.l., Huelva) for the same period as above (2003–2011). For comparison purposes, Figure 3a indicates also the same results for Peñausende-Palencia, including those already shown in Fig. 1. The AOD annual cycle at El Arenosillo was already presented in a former study but for the period 2000–2010 (Bennouna et al., 2011). For the results shown here, due to the end of El Arenosillo site operations in 2010, the time series was extended to 2011 using the data from a new nearby (10 km) AERONET site in Huelva which is meant to replace the El Arenosillo site. As it can be seen, like for Peñausende, at Barcarrota, PM_{10} presents two maxima. At El Arenosillo, the AOD also shows a maximum in March, and two summer maxima in June and August with similar values. Thus, the climatological cycle of AOD/ PM_x is likely to be modulated by African dust intrusion with a south-north gradient. The two maxima in the AOD are separated by a local minimum in July which has been discussed in a number of other studies (Bennouna et al., 2011; Ortiz de Galisteo et al., 2013).

This behavior is consistent with the analysis of the AOD annual cycle attributed to mineral dust transport over the Atlantic using satellite data, which has also shown the presence of several maxima depending on both latitude and longitude (Kaufman et al., 2005). This study extended to a large number of years, should reveal if the bimodality and modulation of the annual cycle for PM_x and AOD is due only to desert dust or if there are other causes, and also how this behavior is distributed over the Iberian Peninsula.

Long-term AOD- PM_x relationships in north-nertral Spain

Y. S. Bennouna et al.

[Title Page](#)[Abstract](#)[Introduction](#)[Conclusions](#)[References](#)[Tables](#)[Figures](#)[Back](#)[Close](#)[Full Screen / Esc](#)[Printer-friendly Version](#)[Interactive Discussion](#)

4.2 Variability and trends

In order to investigate year-to-year variations, Fig. 4 presents the annual cycle of the previous parameters for each year together with the climatological curve as it gets built from the accumulation of prior years. The PM_{10} annual cycle (Fig. 4a) for each year is in general similar to the mean climatological annual cycle, which indicates small shape variations from one year to another, making the accumulated values relatively stable. This can be seen from the “accumulated” curve which changes very little from the first (top) to the last (bottom). The same is also observed when extending the time series back to 2001 when Peñausende started operations. The spring maximum occurs in March for most of the years (2003, 2004, 2005, 2009 and 2010), and a few times in February (2006, 2008), but rarely in April (2011) or May (2007). It should be noted that the spring maximum is much higher in the first years (2003–2005) than later on. In 2009, PM_{10} values are particularly low and no clear maximum appears. In summer, a single peak is usually observed although some years can present two peaks. The absolute maximum in summer is generally observed in August (2003, 2005, 2007, 2008 and 2010), but also in July (2004). For the whole period, the highest peak in summer is observed in July 2004, which corresponds to the strongest desert dust intrusion ever recorded over the Iberian Peninsula (Cachorro et al., 2008). As regards secondary maxima in summer, in general they are found in June (e.g. 2003, 2008). More rarely, peaks can also be found in early-fall such as it is the case in 2008 and 2011.

On the contrary, the annual cycle of the AOD can be very different from one year to another (Fig. 4b), and this can also be observed in the evolution of anomalies in the next Figure. In Fig. 4b, the “accumulated” curve shows two maxima in the first years, but then is smoothed as the position of the maxima moves. Nevertheless, most PM_{10} maxima coincide with those of the AOD. Exceptions are observed though for the years 2007 and 2009, when the spring maximum occurs a month later for the AOD as compared to PM_{10} . The correlation of these monthly means is analyzed in details in Sect. 4.3.

Long-term AOD-PM_x relationships in north-nentral Spain

Y. S. Bennouna et al.

Title Page

Abstract

Introduction

Conclusions

References

Tables

Figures



Back

Close

Full Screen / Esc

Printer-friendly Version

Interactive Discussion



The same monthly means are presented this time to show their evolution in Fig. 5. At first sight, a clear decrease for both the AOD and PM₁₀ can be observed. This can also be seen in the anomaly time series which indicates that from 2008 on, positive anomalies become rare as compared to pre-2008, and hence most monthly anomalies are negative in the last four years. This fact, which has already been noted for the AOD in a previous work (Bennouna et al., 2013) and corroborated here by PM_x data, lead to a trend analysis exercise that was not done in that other paper.

The existence of linear trends in PM_x and AOD data has been tested using the rank-based non-parametric Seasonal Kendall Trend Test (SKTT) using the implementation for MATLAB “Mann–Kendall Test with Sen’s Slope Method for data with Serial Dependence” provided by Jeff Burkey (<http://www.mathworks.com>). The SKTT is an extended version of the standard Mann–Kendall, also called Kendall’s tau test (Mann, 1945; Kendall, 1975; Hirsch and Slack, 1984), which is robust in the case of data presenting strong seasonality. To quantify the magnitude of these trends, this analysis was therefore applied on the monthly values. All the results for the slopes and their associated significance (p value) are reported in Table 6.

Based on all available PM data (2001–2011), it was found that PM₁₀ decreases at a significant rate/slope of $0.42 \mu\text{g m}^{-3} \text{ year}^{-1}$, and this would represents a 31 % reduction during the full period 2001–2011. In the case of PM_{2.5} the trend calculation leads to a significant rate/slope of $0.38 \mu\text{g m}^{-3} \text{ year}^{-1}$, and thus a reduction of 43 % over the full period. This result is in perfect agreement with (Cusack et al., 2012) for the same site but during a slightly shorter period (2002–2010), finding a reduction of 42 % for PM_{2.5}. However, for the coarse mass fraction or PM_{2.5–10}, the weak negative slope that is found here is not significant (see Table 6). In a previous study on the same period but ending a year earlier, (Barnpadimos et al., 2012) also found a lack of significance in the trend for the coarse particles. As regards the AOD prior to the calculation of the trend slope, missing monthly means had to be completed. Most missing months could be filled by the use of Autila data, and the two missing months that remain (one in 2006 and the other in 2010) were replaced by long term average values, i.e. monthly means

of the climatological annual cycle presented above. During the period 2001–2011, the AOD also presents a statistically significant decreasing trend of 0.0041 per year.

The decreasing trend is also clearly noticeable in Fig. 6a and Table 4 when looking directly at the annual averages of PM_{10} , decreasing from $15.1 \mu\text{g m}^{-3}$ in 2001 to $10.1 \mu\text{g m}^{-3}$ in 2011 (i.e. 33 % reduction). Besides, the variations of $PM_{2.5}$ annual mean are again similar to those of PM_{10} , which is decreasing from $9.9 \mu\text{g m}^{-3}$ in 2001 to $5.2 \mu\text{g m}^{-3}$ in 2011 (cf. Fig. 6 and Table 5). However, this graph reveals a new behavior which was not obvious in the previous monthly timeseries, as it seems that the trend slope is inverted in the last 3–4 year. For PM_x data it is not so clear when the slope inversion takes place but it seems to be rather between 2008–2010. For AOD data the trend change is much clearer as shown by the steep slopes around the minimum value, which according to the AOD curve might be taking place in 2009 or 2010. To make an appropriate recalculation of the trend for the adequate period, a more accurate determination of the location of this minimum is needed. The method proposed to resolve this problem is illustrated in subsequent findings.

With Fig. 6b, it is intended to estimate the contribution of the desert dust aerosol to the decreasing trend that is observed. The contribution is obtained by doing the difference between the quantities calculated including and excluding days with desert dust aerosols. The days with desert dust aerosols have been identified using the inventory of desert dust event carried out by Cachorro et al. (2013) for the period 2003–2011, which is based on a manual inspection of both AOD (at Palencia and Autilla) and PM_x (at Peñausende) with the support of other sources of information such as backtrajectories, satellite images, synoptic maps and forecasts from transport models.

As it can be seen, the contribution of desert dust aerosols to the total aerosol load provides consistent results for PM_{10} and AOD. According to PM_{10} , since the beginning of the period, the contribution of desert dust aerosol has been decreasing from nearly 20 % to as low as 7 % in 2009, when it seems to start a slight increase in the last years (2010–2011). To this concern, it should be highlighted that in a study for the Mediterranean basin, Pey et al. (2013) found a clear and persistent anomaly in the

Long-term AOD- PM_x relationships in north-central Spain

Y. S. Bennouna et al.

Title Page

Abstract

Introduction

Conclusions

References

Tables

Figures



Back

Close

Full Screen / Esc

Printer-friendly Version

Interactive Discussion



North Atlantic Oscillation (NAO) index starting in 2006, which is consistently correlated with the trends observed in PM_X , and in particular in North-East Spain. Such a negative anomaly revealed by the NAO index has not been observed since the 1950s.

For the AOD, the variations are similar except for years 2005 and 2006 where the contribution drops suddenly from 20 % to less than 10 %, whereas PM_{10} contribution remains relatively high with a magnitude close to that of the previous years. For 2006, this can be easily explained by the fact that almost two complete months of data are missing and precisely the months of June and July. These months known to be often affected by desert dust intrusion are critical for the representativity of the annual mean and for this reason, the obtained contribution to the AOD is lower than it should be actually. This is demonstrated in Fig. 7a which shows that when using only coinciding daily data series for all parameters, the agreement between dust contributions to PM_X and AOD is significantly improved for 2006.

In 2005, the problem is slightly different because it is related this time to a strong desert dust event. During this episode, which took place on 19 and 20 March 2005, PM_{10} records present an extremely high value of 112 and 143 $\mu\text{g m}^{-3}$ respectively, and it must be highlighted that such a strong event represents no less than 38 % of the annual contribution of desert dust, and therefore can affect considerably the result. Despite such records of PM_{10} , it was found that the AOD at 440 nm remains at the value of 0.21 and 0.26 ($\alpha = 0.38, 0.29$) for those days, which does not reflect the intensity of the intrusion. Indeed, as a comparison, it could be mentioned that for the 24 and 25 July 2004, PM_{10} data was as high as 197 and 130 $\mu\text{g m}^{-3}$ respectively, with corresponding AOD (440 nm) of 0.89 and 0.75 ($\alpha = 0.11, 0.19$) (Cachorro et al., 2008). However, 19 and 20 March 2005 were particularly cloudy, and only few AOD measurements were available. The poor sampling and possible failure of the cloud screening therefore explains the inconsistently low value of the AOD. Figure 7b and c confirm that this fact partly explains the difference observed in 2005. Indeed, when restricting to the use of coinciding daily data series for all parameters in addition of removing the March 2005 event from the timeseries, or correcting aforementioned AOD values to

Long-term AOD- PM_X relationships in north-nentral Spain

Y. S. Bennouna et al.

[Title Page](#)[Abstract](#)[Introduction](#)[Conclusions](#)[References](#)[Tables](#)[Figures](#)[Back](#)[Close](#)[Full Screen / Esc](#)[Printer-friendly Version](#)[Interactive Discussion](#)

Long-term AOD-PM_x relationships in north-central Spain

Y. S. Bennouna et al.

Title Page

Abstract

Introduction

Conclusions

References

Tables

Figures



Back

Close

Full Screen / Esc

Printer-friendly Version

Interactive Discussion



more realistic ones (AOD (440 nm)~ 0.8), all contributions curves agree better. Hence, the difference observed in 2005 results from a combination of sampling issues at different time scales. On one hand daily sampling of the AOD leads to missing days in the timeseries, and on the other hand instantaneous sampling of the AOD leads to an unrealistic representation of one of the strongest events of that year.

To sum up on the disagreements found for both years 2005 and 2006, it appears obvious that PM_x data are more reliable than AOD data for the trend analysis due to sampling issues. However, when these issues are artificially overcome, it is important to point out the remarkable agreement in the long-term evolution of the desert dust contribution for all parameters which is obtained here.

Given these very last results, the trends were newly calculated with the same method as above, but this time for different periods ending in 2009 where the minimum of desert dust contribution to the annual mean was found for all parameters. The reason for taking several different periods instead of simply calculating the trend back to the beginning of the dataset, is to make sure there is consistency between PM_x dataset and AOD dataset since one starts a few years earlier than the other. Consequently the trend calculations for PM_x data were not only performed for 2001–2011 and 2001–2009, but also for 2003–2009 and 2003–2011, as shown in Table 6. It is found here, as expected, that there is no inconsistency in PM_x when comparing the trend results for the two periods ending in 2011 and starting either in 2001 or 2003. In these cases, for each parameter, the results on both slopes and associated *p* values are sensibly similar. The same is observed when comparing periods 2001–2009 with 2003–2009, though the slopes are slightly smaller when a fewer number of years is considered. Therefore there is only little influence on the trend calculation when using a dataset starting in 2003 instead of 2001. The trends calculated from the AERONET dataset can thus be related to those obtained with the EMEP dataset even if the former records start 3 years later than the latter. However, the trend results become different when the periods end in 2009 instead of 2011. Indeed, as expected from the previous results, the slopes are slightly larger than those ending in 2011 because the trend inversion was taken into

Long-term AOD-PM_x relationships in north-central Spain

Y. S. Bennouna et al.

Title Page

Abstract

Introduction

Conclusions

References

Tables

Figures



Back

Close

Full Screen / Esc

Printer-friendly Version

Interactive Discussion



account. But the most interesting result is to notice that the trends become more significant when considering periods ending in 2009 as compared to those ending in 2011. Hence, this corroborates again and in another way the existence of a trend inversion in 2009. The best trend estimation considered here corresponds to the most significant decrease with rate values of $0.49 \mu\text{g m}^{-3} \text{ year}^{-1}$, $0.37 \mu\text{g m}^{-3} \text{ year}^{-1}$ and 0.005 per year, for PM₁₀, PM_{2.5} and AOD parameters respectively. Although and as it is the case also for all other parameters, ρ values are decreasing for PM_{2.5–10}, for periods ending in 2009, the corresponding slopes obtained remain insignificant in all cases. For PM_{2.5–10}, the lowest ρ value and the largest slope is found for 2001–2009, with $\rho = 0.19$ and $s = -0.07$. This might be explained by the uncertainty on PM_{2.5–10} parameter, first because the coarse particles represent a very small portion of PM₁₀, and second because the values of PM₁₀ recorded at Palencia from which PM_{2.5–10} values are derived, are often particularly low in a region under such clean conditions (see also below sections). As a result, the values obtained for PM_{2.5–10} are often close to the limit of detection and therefore subject to large uncertainties.

4.3 Relations PM₁₀-PM_{2.5}, PM_x-AOD and PM_{2.5}/PM₁₀-Alpha

Figure 8 shows the scatterplot of PM₁₀ and PM_{2.5} data measured at Peñausende. Daily PM₁₀ and PM_{2.5} data are strongly associated with a correlation coefficient of 0.87 and a slope of 1.63, due to the rural and remote character of the station. It is also important here to notice the presence of several isolated points with very high PM₁₀ levels ($> 50 \mu\text{g m}^{-3}$) which correspond to strong desert dust intrusions. The same graph is shown for the monthly means in Fig. 8b, and an even higher correlation coefficient of 0.93 is found with a similar value of 1.51 for the slope. For the coarse mass fraction in Fig. 8c and d, the correlation and slope results are similar to those obtained for the fine fraction. This graph also shows that a single type of aerosol is likely to contribute substantially to the coarse mode fraction, the cloud of points being particularly tightened around the regression line as compared to PM_{2.5}. The large offset obtained here

as compared to $PM_{2.5}$, suggests that there is always a remaining fine mode aerosol in the background air.

The relationship between PM_{10} and AOD is presented in Fig. 9. As expected, these two parameters are found to be moderately correlated (Fig. 9a) with a correlation coefficient of 0.56 for the daily data lying between the 95 % confidence interval (0.53–0.59). It should be noted that although the linear regression was not constrained to pass through the origin, the value at the origin falls within the error limits of PM_x measurements. The correlation is improved when considering the monthly means (Fig. 9b) rising up to 0.70. Here, it must be noted that the monthly means were computed using all available daily data from the individual datasets. When these monthly means are calculated using only coinciding days, the obtained results are sensibly the same ($R = 0.69$, $Y = 58.2X + 2.9$), and therefore are not affected by the sampling difference in the daily data.

Scatter diagrams of AOD vs. Alpha help to identify the aerosol type referring to the climatological aerosol models e.g. continental, desert, maritime, biomass burning (Eck et al., 1999; Vergaz, 2001). The classification of aerosol types in a given area can be based on different criteria depending on the characteristics of the location, e.g. geographical situation, emission sources (Hess et al., 1998; Dubovik et al., 2002; Vergaz et al., 2005; Toledano et al., 2007a). Figure 10 presents the scatterplot of Alpha (440 nm) vs. AOD (440 nm) for the site of Palencia, both for daily averages in Fig. 10a and c and instantaneous measurements (every 15 min) in Fig. 10b, d. In addition, the corresponding range of PM_{10} (Fig. 10a and c) and fine-PM ratio (Fig. 10b and d) is also represented by the colorscale. Here the fine-PM ratio refers to the ratio of $PM_{2.5}$ with respect to PM_{10} . It should be noted that in instantaneous graphs (Fig. 10c and d), for a given day the same value of PM_x and $PM_{2.5}/PM_{10}$ ratio is used for each AOD-Alpha point of the day, PM_x data being available on a daily basis. As regards ratio plots, the number N of data appear different than in PM_{10} plots. The reason for this is that 2 data with ratios above 1 and also a few data which were not consistent with AOD-Alpha information were removed.

Long-term AOD- PM_x relationships in north-nertral Spain

Y. S. Bennouna et al.

[Title Page](#)[Abstract](#)[Introduction](#)[Conclusions](#)[References](#)[Tables](#)[Figures](#)[Back](#)[Close](#)[Full Screen / Esc](#)[Printer-friendly Version](#)[Interactive Discussion](#)

Long-term AOD-PM_x relationships in north-nentral Spain

Y. S. Bennouna et al.

Title Page

Abstract

Introduction

Conclusions

References

Tables

Figures



Back

Close

Full Screen / Esc

Printer-friendly Version

Interactive Discussion



As it can be seen, most AOD-Alpha daily averages (65%) are in the range of 0.0–0.2 and 1.0–2.0 respectively (see also Fig. 12a and d), which are typical of a clean continental area. For low values of the AOD (< 0.10), PM_{10} is generally below $10 \mu\text{g m}^{-3}$ (Fig. 10a). The highest values of PM_{10} ($> 80 \mu\text{g m}^{-3}$) are found for Alpha values below 0.5 and high AODs which correspond to intense desert dust intrusions. As shown in Fig. 10b, these episodes are also associated with the lowest $PM_{2.5}/PM_{10}$ ratio values (0.3–0.4), which can also be observed for Alpha up to 0.7. For Alpha values above 1, the ratio values are usually above 0.4. However between 0.7 and 1.5, the ratio spans over a wide range of values which probably indicate the presence of mixed-aerosol (Desert–Continental) and aged-desert resulting from recirculation processes. However due to the sparcity of daily data, it is easier to identify the different types of aerosols when looking at the instantaneous plots. In particular, the horizontal branches associated with the desert dust aerosols (in the lower part) and the biomass burning (in the upper part) appear more clearly in Fig. 10c and d. For more details on the distribution of the different types of events over time, these graphs are also provided by years in the Appendix to this paper (Figs. B1 and B2).

In Fig. 11a, both PM_{10} and $PM_{2.5}$ are represented as a function of the binned AOD at 440 nm, in the interval 0–1 by steps of 0.05, using the 1698 coinciding data. Each point of the curve corresponds to the mean of PM_x for a given bin of AOD, and the associated standard deviation is represented by vertical bars. Before commenting the results of this figure, it should be noted that the apparent increase of the fine-PM ratio in the first AOD bin is an artefact of the AERONET data, as AOD values near zero become comparable to the uncertainty of the measurement which is ~ 0.01 at 440 nm. As it can be seen, PM_x increases slowly and regularly as the AOD reaches about 0.2, but above this value small maximums start to appear, one around 0.25 and another at 0.4, the highest peak being found for the AOD bin centered at 0.5 with nearly $50 \mu\text{g m}^{-3}$ and $25 \mu\text{g m}^{-3}$ for PM_{10} and $PM_{2.5}$ respectively. These high AOD values correspond to the occurrence of desert dust intrusions in the area. The existence of a few data with an AOD above 0.7 shown by the frequency histogram, are considered as exceptionally

surface data are highly correlated and other for which deposition breaks down this correlation. However, synergy between surface in situ and columnar remote sensed data demonstrated to provide useful information for the aerosol type characterization, and consistent results have been obtained in that sense when combining primary parameters with derived ones such as fine-PM ratio and Ångström exponent.

The Supplement related to this article is available online at doi:10.5194/amtd-7-5829-2014-supplement.

Acknowledgements. The authors are grateful to EMEP for providing observations from their network. Special thanks also go to NASA/GSFC, PHOTONS/LOA and RIMA/GOA people for their long-standing collaboration and for operating and maintaining the AERONET-EUROPE network. The research leading to these results has received funding from the European Union Seventh Framework Programme (FP7/2007e2013) under grant agreement Nr. 262254 [ACTRIS]. Financial supports from the Spanish MINECO (projects of ref. CGL2011-23413, CGL2012-33576) are also gratefully acknowledged. We also thank the Environmental Council of the CyL Regional Government (Consejería de Medio Ambiente, Junta de Castilla y León) for supporting this research.

References

- Al-Saadi, J., Szykman, J., Pierce, R. B., Kittaka, C., Neil, D., Chu, D. A., Remer, L., Gumley, L., Prins, E., Weinstock, L., Macdonald, C., Wayland, R., Dimmick, F., and Fishman, J.: Improving national air quality forecasts with satellite aerosol observations, *B. Am. Meteorol. Soc.*, 86, 1249–1261, 2005. 5833
- Arruti, A., Fernández-Olmo, I., and Irabien, A.: Impact of the global economic crisis on metal levels in particulate matter (PM) at an urban area in the Cantabria Region (northern Spain), *Environ. Pollut.*, 159, 1129–1135, 2011. 5831

Long-term AOD-PM_x relationships in north-central Spain

Y. S. Bennouna et al.

Title Page

Abstract

Introduction

Conclusions

References

Tables

Figures



Back

Close

Full Screen / Esc

Printer-friendly Version

Interactive Discussion



Long-term AOD-PM_x relationships in north-nentral Spain

Y. S. Bennouna et al.

Title Page

Abstract

Introduction

Conclusions

References

Tables

Figures



Back

Close

Full Screen / Esc

Printer-friendly Version

Interactive Discussion



- Artiñano, B., Querol, X., Salvador, P., Rodríguez, S., Alonso, D. G., and Alastuey, A.: Assessment of airborne particulate levels in Spain in relation to the new EU-directive, *Atmos. Environ.*, 35, S43–S53, 2001. 5834
- 5 Barmpadimos, I., Keller, J., Oderbolz, D., Hueglin, C., and Prévôt, A. S. H.: One decade of parallel fine (PM_{2.5}) and coarse (PM₁₀–PM_{2.5}) particulate matter measurements in Europe: trends and variability, *Atmos. Chem. Phys.*, 12, 3189–3203, doi:10.5194/acp-12-3189-2012, 2012. 5841
- 10 Bennouna, Y., Cachorro, V., Toledano, C., Berjón, A., Prats, N., Fuertes, D., Gonzalez, R., Rodrigo, R., Torres, B., and de Frutos, A.: Comparison of atmospheric aerosol climatologies over southwestern Spain derived from AERONET and MODIS, *Remote Sens. Environ.*, 115, 1272–1284, doi:10.1016/j.rse.2011.01.011, 2011. 5839
- 15 Bennouna, Y., Cachorro, V., Torres, B., Toledano, C., Berjón, A., de Frutos, A., and Alonso Fernández Coppel, I.: Atmospheric turbidity the annual cycle of aerosol optical depth over north-center Spain with ground (AERONET) and satellite (MODIS) remotely sensed data, *Atmos. Environ.*, 67, 352–364, 2013. 5837, 5838, 5841, 5880
- Borowiak, A. and De Saeger E.: Harmonization of air quality measurements at European Union level, *Analyst*, 121, 1247–1248, 1996.
- 20 Brown, J. S., Gordon, T., Price, O., and Asgharian, B.: Thoracic and respirable particle definitions for human health risk assessment, *Particle and Fibre Toxicology*, 2013, 10–12, doi:10.1186/1743-8977-10-12, 2013. 5832
- Cachorro, V. E. and Tanre, D.: The correlation between particle mass loading and extinction: application to desert dust aerosol content estimation, *Remote Sens. Environ.*, 60, 187–194, 1997. 5831
- 25 Cachorro, V. E., Vergaz, R., de Frutos, A. M., Vilaplana, J. M., Henriques, D., Laulainen, N., and Toledano, C.: Study of desert dust events over the southwestern Iberian Peninsula in year 2000: two case studies, *Ann. Geophys.*, 24, 1493–1510, doi:10.5194/angeo-24-1493-2006, 2006. 5833
5834
- 30 Cachorro, V., Toledano, C., Prats, N., Sorribas, M., Mogo, S., Berjón, A., Torres, B., Rodrigo, R., De la Rosa, J., and De Frutos, A.: The strongest desert dust intrusion mixed with smoke over the Iberian Peninsula registered with Sun photometry, *J. Geophys. Res.*, 113, D14S04, doi:10.1029/2007JD009582, 2008. 5834, 5840, 5843, 5848

Long-term AOD-PM_x relationships in north-nentral Spain

Y. S. Bennouna et al.

Title Page

Abstract

Introduction

Conclusions

References

Tables

Figures



Back

Close

Full Screen / Esc

Printer-friendly Version

Interactive Discussion



- Cachorro, V., Burgos, M. A., Bennouna, Y., Toledano, C., Herguedas, A., González Orcajo, J., and de Frutos, A. M.: Inventario del Aerosol Desértico en la Región de Castilla y León (2003–2012), in: Proceedings of the 1st Iberian Meeting Aerosol Science and Technology (RICTA) 2013, (ISBN: 978-989-20-3962-6), 2013. 5838, 5842
- 5 Coz, E., Gómez-Moreno, F. J., Pujadas, M., Casuccio, G. S., Lersch, T. L., and Artíñano, B.: Individual particle characteristics of North African dust under different long-range transport scenarios, *Atmos. Environ.*, 43, 1850–1863, 2009. 5834, 5836
- Cusack, M., Alastuey, A., Pérez, N., Pey, J., and Querol, X.: Trends of particulate matter (PM_{2.5}) and chemical composition at a regional background site in the Western Mediterranean over the last nine years (2002–2010), *Atmos. Chem. Phys.*, 12, 8341–8357, doi:10.5194/acp-12-8341-2012, 2012. 5831, 5841
- 10 Dayan, U. and Miller, J.: Meteorological and Climatological Data From Surface and Upper Air Measurements for the Assessment of Atmospheric Transport and Deposition of Pollutants in the Mediterranean Basin: a Review, Tech. rep., Map technical Reports Series, vol. 30 UNEP, WMO (1989), 137 pp., 1989. 5838
- 15 Del Rio, S., Fraile, R., Herrero, L., and Penas, A.: Analysis of recent trends in mean maximum and minimum temperatures in a region of the NW of Spain (Castilla y León), *Theor. Appl. Climatol.*, 90, 1–12, 2007. 5835
- Dubovik, O., Holben, B., Eck, T. F., Smirnov, A., Kaufman, Y. J., King, M. D., Tanré, D., and Slutsker, I.: Variability of absorption and optical properties of key aerosol types observed in worldwide locations, *J. Atmos. Sci.*, 59, 590–608, 2002. 5846
- EC: Directive 1999/30/EC of the European Parliament and of the Council (22 April 1999) relating to limit values for sulphur dioxide and oxides of nitrogen, PM and lead in ambient air, *Official Journal of the European Communities*, L 163, 41–60, 1999. 5832
- 25 EC: Directive 2008/50/EC of the European Parliament and of the Council (21 May 2008) on Ambient Air Quality and Cleaner Air for Europe, *Official Journal of the European Communities*, L 151, 1–44, 2008. 5831, 5832
- Eck, T., Holben, B., Reid, J., Dubovik, O., Smirnov, A., O'Neill, N., Slutsker, I., and Kinne, S.: Wavelength dependence of the optical depth of biomass burning, urban, and desert dust aerosols, *J. Geophys. Res.*, 104, 31333–31349, 1999. 5837, 5846
- 30 EMEP: EMEP/CCC-Report 1/95, EMEP Manual for Sampling and Chemical Analysis, rev 2002, Norwegian Institute for Air Research, available at:

Long-term AOD-PM_x relationships in north-nentral Spain

Y. S. Bennouna et al.

Title Page

Abstract

Introduction

Conclusions

References

Tables

Figures



Back

Close

Full Screen / Esc

Printer-friendly Version

Interactive Discussion



a federated instrument network and data archive for aerosol characterization, *Remote Sens. Environ.*, 66, 1–16, 1998. 5832, 5836

Holben, B., Tanre, D., Smirnov, A., Eck, T., Slutsker, I., Abuhassan, N., Newcomb, W., Schafer, J., Chatenet, B., Lavenu, F., Kaufman, Y. J., Vande Castle, J., Setzer, A., Markham, B., Clark, D., Frouin, R., Halthore, R., Karneli, A., O'Neill, N. T., Pietras, C., Pinker, R. T., Voss, K., and Zibordi, G.: An emerging ground-based aerosol climatology: aerosol optical depth from AERONET, *J. Geophys. Res.-Atmos.*, 106, 12067–12097, 2001. 5832

Kaufman, Y., Koren, I., Remer, L., Tanré, D., Ginoux, P., and Fan, S.: Dust transport and deposition observed from the Terra-Moderate Resolution Imaging Spectroradiometer (MODIS) spacecraft over the Atlantic Ocean, *J. Geophys. Res.*, 110, D10S12, doi:10.1029/2003JD004436, 2005. 5839

Kendall, M. G.: *Rank Correlation Methods*, Griffin, London, 1975. 5841

King, M. D., Kaufman, Y. J., Tanré, D., and Nakajima, T.: Remote sensing of tropospheric aerosols from space: past, present, and future, *B. Am. Meteorol. Soc.*, 80, 2229–2259, 1999. 5833

Koelemeijer, R., Homan, C., and Matthijsen, J.: Comparison of spatial and temporal variations of aerosol optical thickness and particulate matter over Europe, *Atmos. Environ.*, 40, 5304–5315, 2006. 5833

Kokhanovsky, A., Breon, F.-M., Cacciari, A., Carboni, E., Diner, D., Di Nicolantonio, W., Grainger, R., Grey, W., Höller, R., Lee, K.-H., Li, Z., North, P. R. J., Sayer, A. M., Thomas, G. E., and von Hoyningen-Huene, W.: Aerosol remote sensing over land: a comparison of satellite retrievals using different algorithms and instruments, *Atmos. Res.*, 85, 372–394, 2007. 5833

Kokhanovsky, A. A., Prikhach, A. S., Katsev, I. L., and Zege, E. P.: Determination of particulate matter vertical columns using satellite observations, *Atmos. Meas. Tech.*, 2, 327–335, doi:10.5194/amt-2-327-2009, 2009. 5833

Liu, Y., Koutrakis, P., and Kahn, R.: Estimating fine particulate matter component concentrations and size distributions using satellite-retrieved fractional aerosol optical depth: Part 1 – method development, *J. Air Waste Manage.*, 57, 1351–1359, 2007a. 5833

Liu, Y., Koutrakis, P., Kahn, R., Turquety, S., and Yantosca, R. M.: Estimating fine particulate matter component concentrations and size distributions using satellite-retrieved fractional aerosol optical depth: Part 2 – a case study, *J. Air Waste Manage.*, 57, 1360–1369, 2007b. 5833

Long-term AOD-PM_x relationships in north-central Spain

Y. S. Bennouna et al.

Title Page

Abstract

Introduction

Conclusions

References

Tables

Figures



Back

Close

Full Screen / Esc

Printer-friendly Version

Interactive Discussion



Lyamani, H., Olmo, F., and Alados-Arboledas, L.: Saharan dust outbreak over southeastern Spain as detected by sun photometer, *Atmospheric Environment*, 39, 7276–7284, 2005. 5834

Lyamani, H., Olmo, F., Foyo, I., and Alados-Arboledas, L.: Black carbon aerosols over an urban area in south-eastern Spain: changes detected after the 2008 economic crisis, *Atmos. Environ.*, 45, 6423–6432, 2011. 5831

Mann, H. B.: Nonparametric tests against trend, *Econometrica*, 13, 245–259, 1945. 5841

Ortiz de Galisteo, J. P., Bennouna, Y., Toledano, C., Cachorro, V., Romero, P., Andrés, M. I., and Torres, B.: Analysis of the annual cycle of the precipitable water vapour over Spain from 10-year homogenized series of GPS data, *Q. J. R. Meteorol. Soc.*, 140, 397–406, doi:10.1002/qj.2146, 2013. 5839

Osornio-Vargas, A. R., Serrano, J., Rojas-Bracho, L., Miranda, J., García-Cuellar, C., Reyna, M. A., Flores, G., Zuk, M., Quintero, M., Vázquez, I., Sánchez-Pérez, Y., López, T., and Rosas, I.: In vitro biological effects of airborne PM_{2.5} and PM₁₀ from a semi-desert city on the Mexico-US border, *Chemosphere*, 83, 618–626, 2011. 5831

Pelletier, B., Santer, R., and Vidot, J.: Retrieving of particulate matter from optical measurements: a semiparametric approach, *J. Geophys. Res.*, 112, D06208, doi:10.1029/2005JD006737, 2007. 5833

Pey, J., Querol, X., Alastuey, A., Forastiere, F., and Stafoggia, M.: African dust outbreaks over the Mediterranean Basin during 2001–2011: PM₁₀ concentrations, phenomenology and trends, and its relation with synoptic and mesoscale meteorology, *Atmos. Chem. Phys.*, 13, 1395–1410, doi:10.5194/acp-13-1395-2013, 2013. 5842

Pinto, M., Labajo, J. L., and Piorno, A.: Atmospheric Pressure Trends between 1945 and 1994 in Castilla and León (Spain), *Detecting and Modelling Regional Climate Change*, 239 pp., 2001. 5835

Pope III, C. A.: Review: epidemiological basis for particulate air pollution health standards, *Aerosol Sci. Tech.*, 32, 4–14, 2000. 5830

Querol, X., Alastuey, A., Rodriguez, S., Viana, M., Artinano, B., Salvador, P., Mantilla, E., do Santos, S., Patier, R., de La Rosa, J., de la Campa, A., Sanchez, Menéndez, M., and Gil, J. J.: Levels of particulate matter in rural, urban and industrial sites in Spain, *Sci. Total Environ.*, 334, 359–376, 2004. 5834

Querol, X., Minguillón, M., Alastuey, A., Monfort, E., Mantilla, E., Sanz, M., Sanz, F., Roig, A., Renau, A., Felis, C., Miró, J. V., and Artíñano, B.: Impact of the implementation of PM

Long-term AOD-PM_x relationships in north-nentral Spain

Y. S. Bennouna et al.

Title Page

Abstract

Introduction

Conclusions

References

Tables

Figures



Back

Close

Full Screen / Esc

Printer-friendly Version

Interactive Discussion



gramme (EMEP) and observed atmospheric composition change during 1972–2009, Atmos. Chem. Phys., 12, 5447–5481, doi:10.5194/acp-12-5447-2012, 2012. 5832

Van Donkelaar, A., Martin, R. V., and Park, R. J.: Estimating ground-level PM_{2.5} using aerosol optical depth determined from satellite remote sensing, J. Geophys. Res., 111, D21201, doi:10.1029/2005JD006996, 2006. 5833

Vergaz, R.: Propiedades ópticas de los aerosoles atmosféricos, Caracterización del área del Golfo de Cádiz, Ph.D. thesis, Universidad de Valladolid, Spain, 2001. 5834, 5846

Vergaz, R., Cachorro, V. E., De Frutos, Á. M., Vilaplana, J. M., and De La Morena, B. A.: Columnar characteristics of aerosols by spectroradiometer measurements in the maritime area of the Cadiz Gulf (Spain), Int. J. Climatol., 25, 1781–1804, 2005. 5834, 5846

Vidot, J., Santer, R., and Ramon, D.: Atmospheric particulate matter (PM) estimation from SeaWiFS imagery, Remote Sens. Environ., 111, 1–10, 2007. 5833

Vrekoussis, M., Richter, A., Hilboll, A., Burrows, J., Gerasopoulos, E., Lelieveld, J., Barrie, L., Zerefos, C., and Mihalopoulos, N.: Economic crisis detected from space: Air quality observations over Athens/Greece, Geophys. Res. Lett., 40, 458–463, 2013. 5831

WHO: Air Quality Guidelines: Global Update 2005: Particulate Matter, Ozone, Nitrogen Dioxide and Sulfur Dioxide, World Health Organization, 2006. 5831

Zhang, H., Hoff, R. M., and Engel-Cox, J. A.: The relation between Moderate Resolution Imaging Spectroradiometer (MODIS) aerosol optical depth and PM_{2.5} over the United States: a geographical comparison by US Environmental Protection Agency regions, J. Air Waste Manage., 59, 1358–1369, 2009. 5833

Long-term AOD-PM_x relationships in north-nentral Spain

Y. S. Bennouna et al.

Table 1. Yearly statistics of EMEP PM₁₀, PM_{2.5}, and AERONET AOD data counts in the region of study for the period 2001–2011. For AOD data counts, one column refers to Palencia records only (3rd column), and the other to Palencia records completed with those of Autila (4th column).

Year	N_{days} (PM ₁₀)	N_{days} (PM _{2.5})	N_{days} (AOD)	N_{days} (AOD')
2001	251 (68.8 %)	251 (68.8 %)	–	–
2002	311 (85.2 %)	311 (85.2 %)	–	–
2003	321 (87.9 %)	321 (87.9 %)	163 (44.7 %)	163 (44.7 %)
2004	334 (91.3 %)	334 (91.3 %)	271 (74.0 %)	271 (74.0 %)
2005	336 (92.1 %)	336 (92.1 %)	295 (80.8 %)	295 (80.8 %)
2006	326 (89.3 %)	326 (89.3 %)	173 (47.4 %)	173 (47.4 %)
2007	330 (90.4 %)	330 (90.4 %)	271 (74.2 %)	271 (74.2 %)
2008	315 (86.1 %)	315 (86.1 %)	266 (72.7 %)	266 (72.7 %)
2009	327 (89.6 %)	327 (89.6 %)	109 (29.9 %)	261 (71.5 %)
2010	347 (95.1 %)	335 (91.8 %)	68 (18.6 %)	242 (66.3 %)
2011	333 (91.2 %)	333 (91.2 %)	226 (61.9 %)	239 (65.5 %)
Average	321.0 (87.9 %)	319.9 (87.6 %)	204.7 (56.0 %)	242.3 (66.4 %)
Total	3531 (87.9 %)	3519 (87.6 %)	1842 (56.0 %)	2181 (66.4 %)

Title Page

Abstract

Introduction

Conclusions

References

Tables

Figures



Back

Close

Full Screen / Esc

Printer-friendly Version

Interactive Discussion



Long-term AOD-PM_x relationships in north-nentral Spain

Y. S. Bennouna et al.

Table 3. Monthly statistics of the EMEP PM_{2.5} for the period 2003–2011, including: the mean (\overline{PM}), the standard deviation (σ), the median (\tilde{PM}), the first and the second quartile (P25 and P75), the 5th and 95th percentiles (P5 and P95), the maximum (max) and the minimum (min) values. The results of the “Total” line are based on all daily values.

Month	N_{days}	PM _{2.5}							
		$\overline{PM} \pm \sigma$	\tilde{PM}	P25	P75	P5	P95	min	max
Jan	225 (81 %)	4.9 ± 3.7	4.0	2.0	6.0	1.0	13.3	1.0	19.0
Feb	225 (89 %)	6.7 ± 5.7	5.0	3.0	9.3	1.0	18.0	1.0	41.0
Mar	259 (93 %)	6.8 ± 5.4	5.0	3.0	9.0	2.0	18.0	1.0	36.0
Apr	242 (90 %)	5.5 ± 3.5	5.0	3.0	7.0	2.0	13.0	1.0	24.0
May	253 (91 %)	7.2 ± 4.7	6.0	4.0	8.3	3.0	17.0	1.0	31.0
Jun	249 (92 %)	8.0 ± 4.4	7.0	5.0	11.0	3.0	17.0	2.0	22.0
Jul	262 (94 %)	9.0 ± 6.3	7.0	5.0	11.0	3.0	20.4	2.0	53.0
Aug	268 (96 %)	9.0 ± 6.6	7.0	5.0	11.0	3.0	20.1	2.0	49.0
Sep	252 (93 %)	7.3 ± 3.6	7.0	4.0	10.0	3.0	14.0	2.0	18.0
Oct	242 (87 %)	5.5 ± 3.5	5.0	3.0	7.0	2.0	12.4	1.0	19.0
Nov	245 (91 %)	4.2 ± 2.8	4.0	2.0	5.0	1.0	11.0	1.0	18.0
Dec	235 (84 %)	4.3 ± 2.9	3.0	2.0	5.0	1.0	10.8	1.0	16.0
Total	2957 (90 %)	6.6 ± 4.9	5.0	3.0	8.0	2.0	16.0	1.0	53.0

Title Page

Abstract

Introduction

Conclusions

References

Tables

Figures



Back

Close

Full Screen / Esc

Printer-friendly Version

Interactive Discussion



Long-term AOD-PM_x relationships in north-nentral Spain

Y. S. Bennouna et al.

Table 4. Yearly statistics of EMEP PM₁₀ for the period 2001–2011, including: the mean (\overline{PM}), the standard deviation (σ), the median (\tilde{PM}), the first and the second quartile (P25 and P75), the 5th and 95th percentiles (P5 and P95), the maximum (max) and the minimum (min) values. The results of the “Total” line are based on all daily values.

Year	N_{days}	$\overline{PM} \pm \sigma$	PM ₁₀						
			\tilde{PM}	P25	P75	P5	P95	min	max
2001	251	15.1 ± 10.0	13.0	9.0	18.0	5.0	34.0	3.0	90.0
2002	311	12.3 ± 9.0	10.0	6.0	15.8	3.0	31.0	1.0	62.0
2003	321	12.9 ± 10.0	10.0	6.0	16.3	3.0	32.5	1.0	62.0
2004	334	13.5 ± 14.8	10.0	7.0	15.0	4.0	30.0	2.0	197.0
2005	336	12.8 ± 12.9	9.0	6.0	16.0	4.0	29.0	2.0	143.0
2006	326	11.3 ± 7.5	10.0	6.0	15.0	3.0	27.2	2.0	49.0
2007	330	10.9 ± 7.8	9.0	6.0	13.0	4.0	23.0	2.0	68.0
2008	315	9.8 ± 6.9	8.0	5.0	12.8	3.0	23.8	1.0	45.0
2009	327	9.0 ± 5.3	8.0	5.0	11.0	3.0	19.2	1.0	34.0
2010	347	8.7 ± 8.3	7.0	5.0	11.0	3.0	18.0	1.0	94.0
2011	333	10.1 ± 6.8	9.0	5.0	12.0	3.0	23.0	1.0	48.0
Total	3531	11.4 ± 9.6	9.0	6.0	14.0	3.0	28.0	1.0	197.0

[Title Page](#)
[Abstract](#)
[Introduction](#)
[Conclusions](#)
[References](#)
[Tables](#)
[Figures](#)
[◀](#)
[▶](#)
[◀](#)
[▶](#)
[Back](#)
[Close](#)
[Full Screen / Esc](#)
[Printer-friendly Version](#)
[Interactive Discussion](#)


Long-term AOD-PM_x relationships in north-nentral Spain

Y. S. Bennouna et al.

Table 6. Trend results for EMEP PM₁₀, PM_{2.5}, PM_{2.5–10} and AERONET AOD (440 nm) data for the full period 2001–2011 and for different relevant sub-periods, including the trend slope s and associated p value obtained with the SKTT trend test.

Period		PM ₁₀	PM _{2.5}	PM _{2.5–10}	AOD
2001–2011	s	–0.419	–0.385	–0.028	–
	p	0.012	0.003	0.422	–
2003–2011	s	–0.427	–0.387	–0.028	–0.004
	p	0.027	0.012	0.549	0.093
2001–2009	s	–0.437	–0.371	–0.063	–
	p	0.034	–0.013	0.195	–
2003–2009	s	–0.498	–0.382	–0.074	–0.005
	p	0.047	0.048	0.279	0.010

[Title Page](#)
[Abstract](#)
[Introduction](#)
[Conclusions](#)
[References](#)
[Tables](#)
[Figures](#)

[Back](#)
[Close](#)
[Full Screen / Esc](#)
[Printer-friendly Version](#)
[Interactive Discussion](#)


Long-term AOD-PM_x relationships in north-nentral Spain

Y. S. Bennouna et al.

Table A1. Monthly statistics of the EMEP PM₁₀ for the period 2001–2011, including: the mean (\overline{PM}), the standard deviation (σ), the median (\tilde{PM}), the first and the second quartile (P25 and P75), the 5th and 95th percentiles (P5 and P95), the maximum (max) and the minimum (min) values. The results of the “Total” line are based on all daily values.

Month	N_{days}	\overline{pm}	σ	$p\tilde{m}$	PM ₁₀					pm_{min}	pm_{max}
					P25	P75	P5	P95			
Jan	248	7.00	4.95	5.00	4.00	9.00	2.00	17.00	1.00	36.00	
Feb	253	9.51	7.00	7.00	5.00	12.25	3.00	24.00	1.00	50.00	
Mar	304	12.28	13.71	8.00	5.00	14.50	3.00	32.30	1.00	143.00	
Apr	299	9.64	6.80	8.00	5.00	12.00	3.00	21.55	1.00	48.00	
May	305	11.71	7.66	10.00	7.00	14.00	4.00	25.75	2.00	68.00	
Jun	303	14.34	8.35	12.00	9.00	18.00	5.00	33.00	3.00	52.00	
Jul	320	15.75	14.79	12.00	9.00	19.00	6.00	32.00	4.00	197.00	
Aug	324	15.87	11.72	12.00	9.00	19.00	6.00	36.00	3.00	94.00	
Sep	308	12.73	6.29	12.00	8.00	15.00	5.00	24.10	3.00	41.00	
Oct	289	10.65	7.39	8.00	6.00	12.25	3.95	27.00	2.00	45.00	
Nov	291	7.59	5.16	6.00	4.00	9.00	3.00	15.00	1.00	49.00	
Dec	287	7.63	7.42	6.00	4.00	9.00	2.00	19.00	1.00	90.00	
Total	3531	11.40	9.59	9.00	6.00	14.00	3.00	28.00	1.00	197.00	

Title Page

Abstract

Introduction

Conclusions

References

Tables

Figures



Back

Close

Full Screen / Esc

Printer-friendly Version

Interactive Discussion



Long-term AOD-PM_x relationships in north-nentral Spain

Y. S. Bennouna et al.

Table A2. Monthly statistics of the EMEP PM_{2.5} for the period 2001–2011, including: the mean (\overline{PM}), the standard deviation (σ), the median (\tilde{PM}), the first and the second quartile (P25 and P75), the 5th and 95th percentiles (P5 and P95), the maximum (max) and the minimum (min) values. The results of the “Total” line are based on all daily values.

Month	N_{days}	\overline{pm}	σ	$p\tilde{m}$	PM _{2.5}		P5	P95	pm_{min}	pm_{max}
					P25	P75				
Jan	247	5.04	3.85	4.00	2.00	6.00	1.00	14.00	1.00	20.00
Feb	251	6.80	5.54	5.00	3.00	9.00	1.00	17.90	1.00	41.00
Mar	302	6.94	5.41	5.00	3.00	9.00	2.00	18.00	1.00	36.00
Apr	297	6.17	4.09	5.00	3.00	8.00	2.00	14.00	1.00	28.00
May	304	7.29	4.73	6.00	4.00	9.00	3.00	17.00	1.00	31.00
Jun	303	8.72	5.00	8.00	5.00	12.00	3.00	18.00	2.00	37.00
Jul	319	9.43	6.40	8.00	5.00	12.00	3.00	21.00	2.00	53.00
Aug	324	9.49	6.68	8.00	5.00	11.50	3.00	21.00	2.00	49.00
Sep	307	7.60	4.13	7.00	4.00	10.00	3.00	14.00	2.00	31.00
Oct	288	5.69	3.62	5.00	3.00	7.50	2.00	13.00	1.00	19.00
Nov	291	4.47	2.92	4.00	2.00	5.00	1.00	11.00	1.00	18.00
Dec	286	4.95	4.03	4.00	2.00	6.00	1.00	14.00	1.00	25.00
Total	3519	6.97	5.13	6.00	3.00	9.00	2.00	16.00	1.00	53.00

Title Page

Abstract

Introduction

Conclusions

References

Tables

Figures



Back

Close

Full Screen / Esc

Printer-friendly Version

Interactive Discussion



Long-term AOD-PM_x relationships in north-central Spain

Y. S. Bennouna et al.

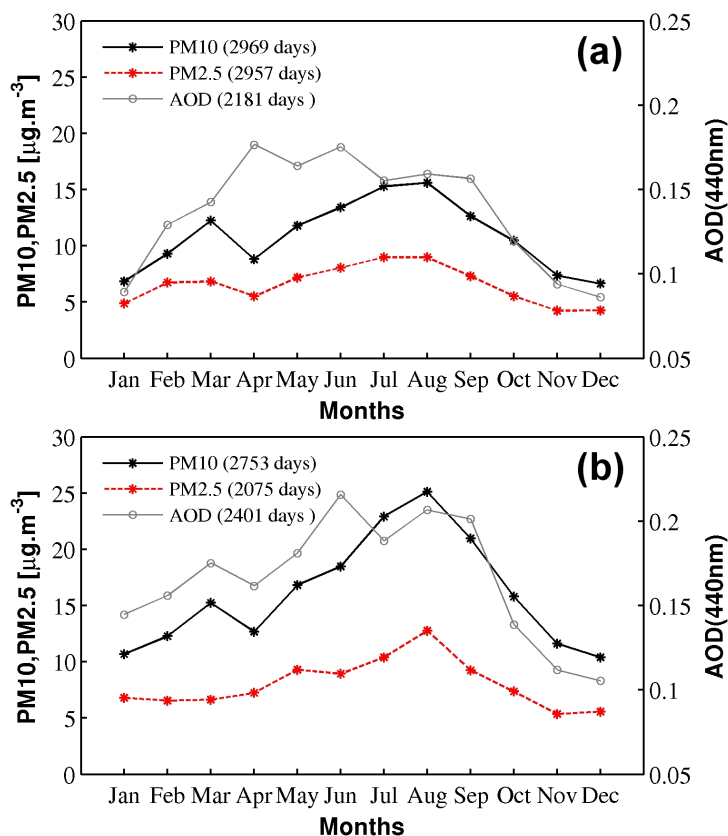


Figure 3. Mean annual cycle of the AOD (440 nm), PM₁₀ and PM_{2.5} for two representative regions of the Iberian Peninsula: **(a)** the north-central area the sites Peñausende (EMEP) and Palencia (AERONET) **(b)** the southwestern area with the sites Barcarrota (EMEP) and El Arenosillo (AERONET), during the period 2003–2011.

Long-term AOD-PM_x relationships in north-nentral Spain

Y. S. Bennouna et al.

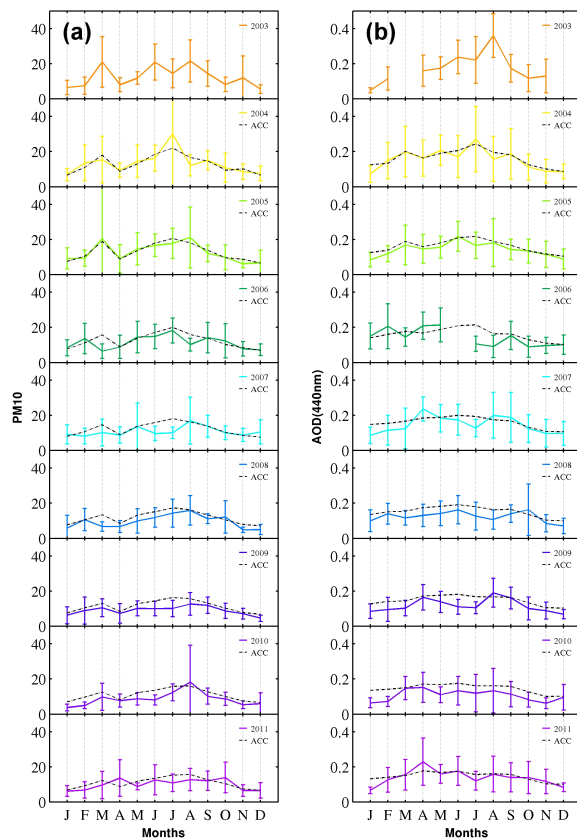


Figure 4. Mean annual cycle of (a) PM₁₀ data and (b) AOD (440 nm), derived for each year (color solid line) and for cumulative multi-annual periods (black dotted line). The error bars represent the standard deviation of the daily data for a given month-year. The black dotted line of the bottom graphs corresponds to the annual cycle based on the entire period 2003–2011 that is also shown on Fig. 1.

[Title Page](#)
[Abstract](#)
[Introduction](#)
[Conclusions](#)
[References](#)
[Tables](#)
[Figures](#)

[Back](#)
[Close](#)
[Full Screen / Esc](#)
[Printer-friendly Version](#)
[Interactive Discussion](#)


Long-term AOD-PM_x relationships in north-nentral Spain

Y. S. Bennouna et al.

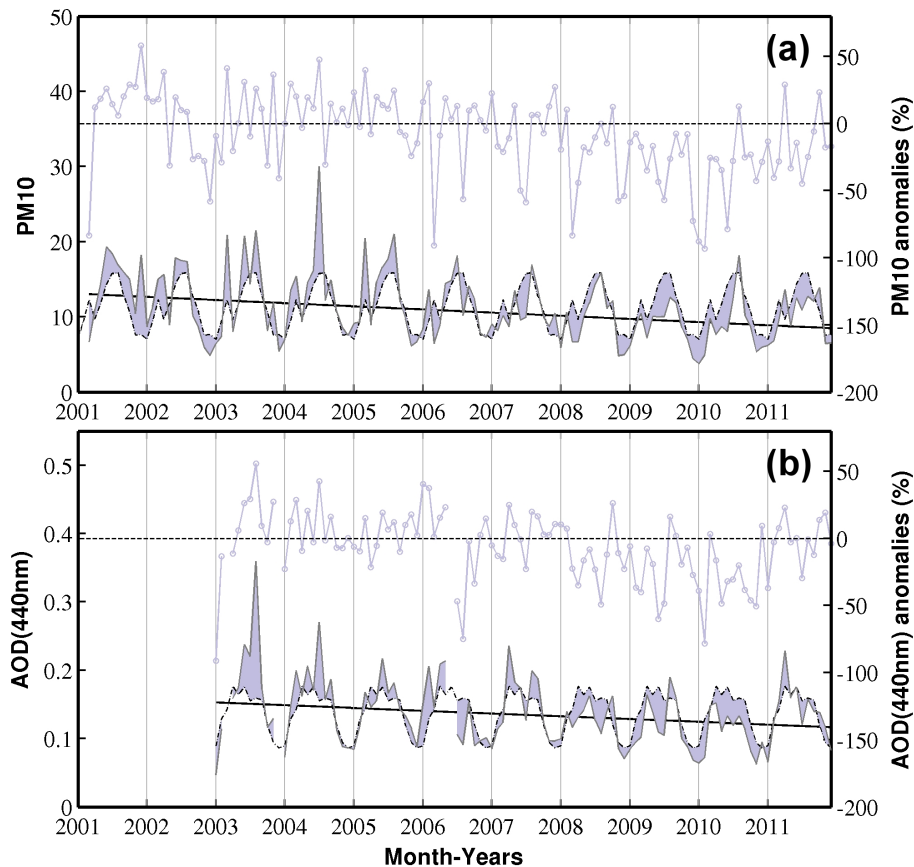


Figure 5. Evolution of the monthly means (right axis) and associated relative anomalies (right axis) between 2001 and 2011 for **(a)** PM₁₀ and **(b)** AOD (440 nm) with respect to the mean annual cycle calculated over the entire period. The latter is also represented by a dash-dotted curve. The solid line indicates the trends obtained with the Seasonal Kendall Trend Test for the full period (see also Table 6).

Title Page

Abstract

Introduction

Conclusions

References

Tables

Figures



Back

Close

Full Screen / Esc

Printer-friendly Version

Interactive Discussion



Long-term AOD-PM_x relationships in north-nentral Spain

Y. S. Bennouna et al.

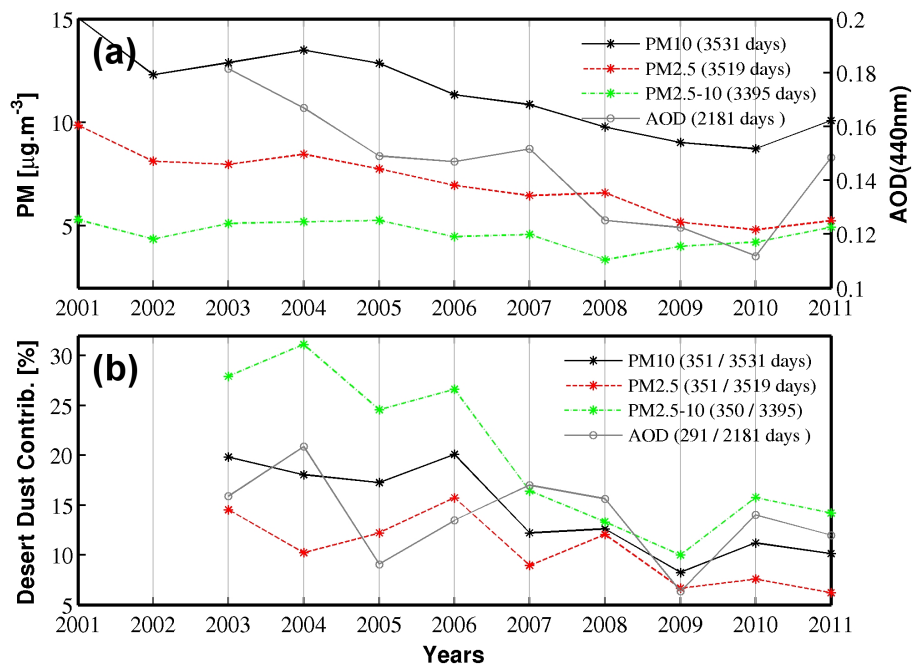


Figure 6. Evolution of (a) the annual means and (b) associated desert dust aerosol contribution between 2001/2003 and 2011 for the AOD (440 nm), PM₁₀, PM_{2.5} and PM_{2.5-10}.

Title Page

Abstract

Introduction

Conclusions

References

Tables

Figures

◀

▶

◀

▶

Back

Close

Full Screen / Esc

Printer-friendly Version

Interactive Discussion



Long-term AOD-PM_x relationships in north-central Spain

Y. S. Bennouna et al.

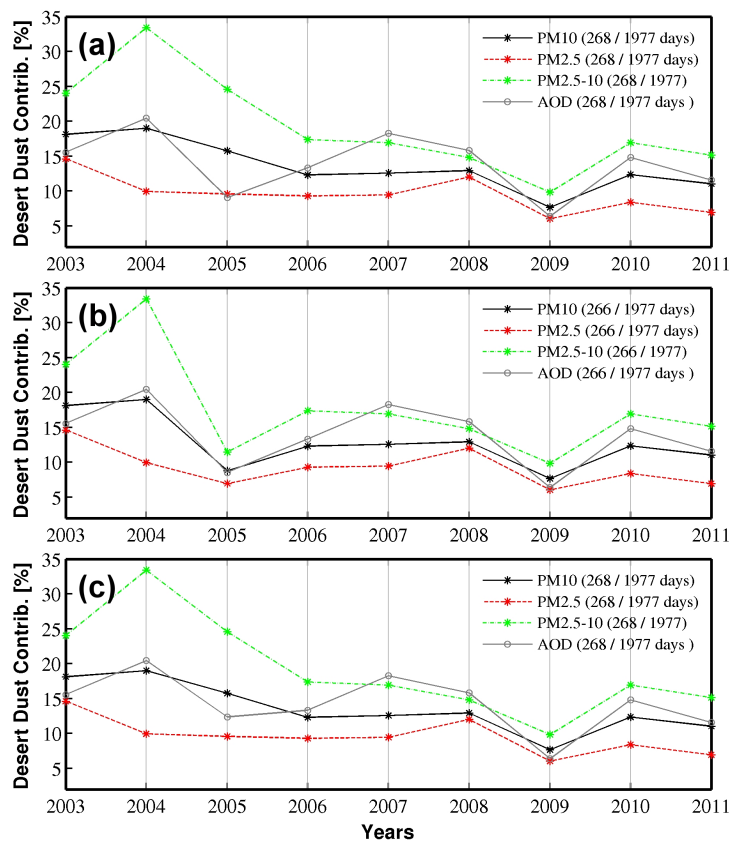


Figure 7. Same as Fig. 6a in the case of **(a)** considering only coincident daily data for all time series, **(b)** same as **(a)** but removing the daily data corresponding to the dust event of March 2005, and **(c)** same as **(a)** but modifying the AOD daily data corresponding to the dust event of March 2005 to more realistic values.

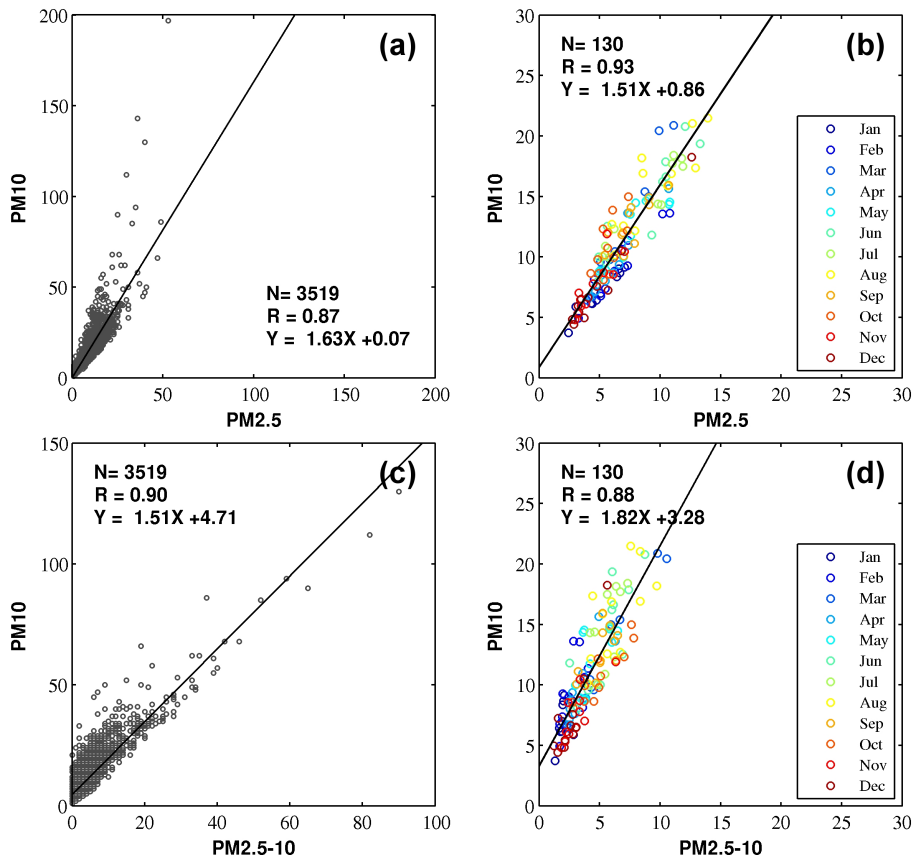


Figure 8. Scatterplots PM₁₀ vs. PM_{2.5} and vs. PM_{2.5-10}, for (a, c) daily values and (b, d) monthly means, corresponding to the period 2001–2011.

**Long-term AOD-PM_x
relationships in
north-nentral Spain**

Y. S. Bennouna et al.

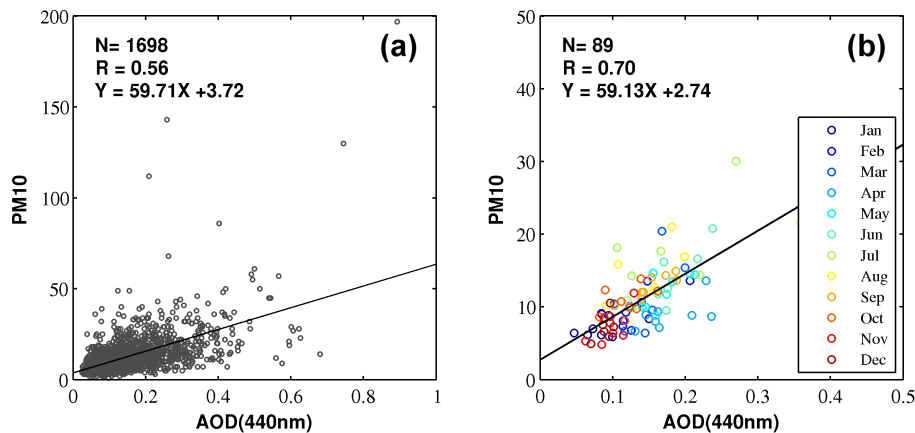


Figure 9. Scatterplots PM₁₀ vs. AOD (440 nm) for **(a)** daily values and **(b)** monthly means, corresponding to the period 2003–2011.

[Title Page](#)[Abstract](#)[Introduction](#)[Conclusions](#)[References](#)[Tables](#)[Figures](#)[Back](#)[Close](#)[Full Screen / Esc](#)[Printer-friendly Version](#)[Interactive Discussion](#)

Long-term AOD-PM_x
relationships in
north-nentral Spain

Y. S. Bennouna et al.

Title Page

Abstract

Introduction

Conclusions

References

Tables

Figures



Back

Close

Full Screen / Esc

Printer-friendly Version

Interactive Discussion

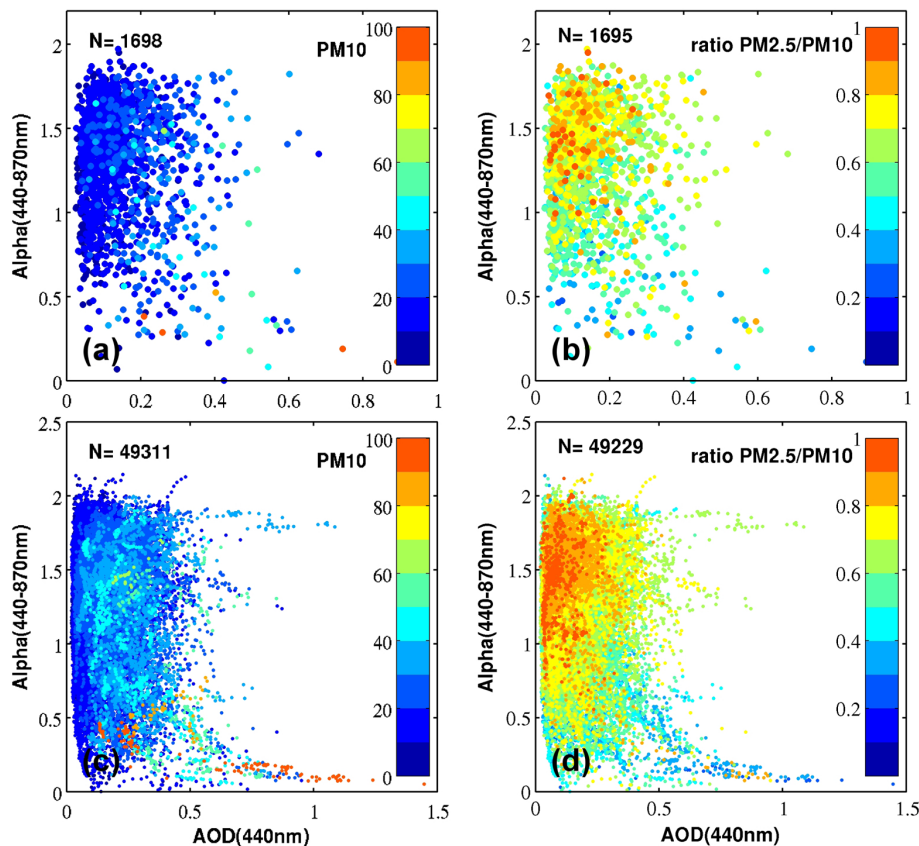


Figure 10. Scatterplots Alpha (440–870 nm) vs. AOD (440 nm) for daily (a, b) and instantaneous data (c, d) with corresponding range of (a, c) PM₁₀ and (b, d) fine-PM ratio for the period 2003–2011.

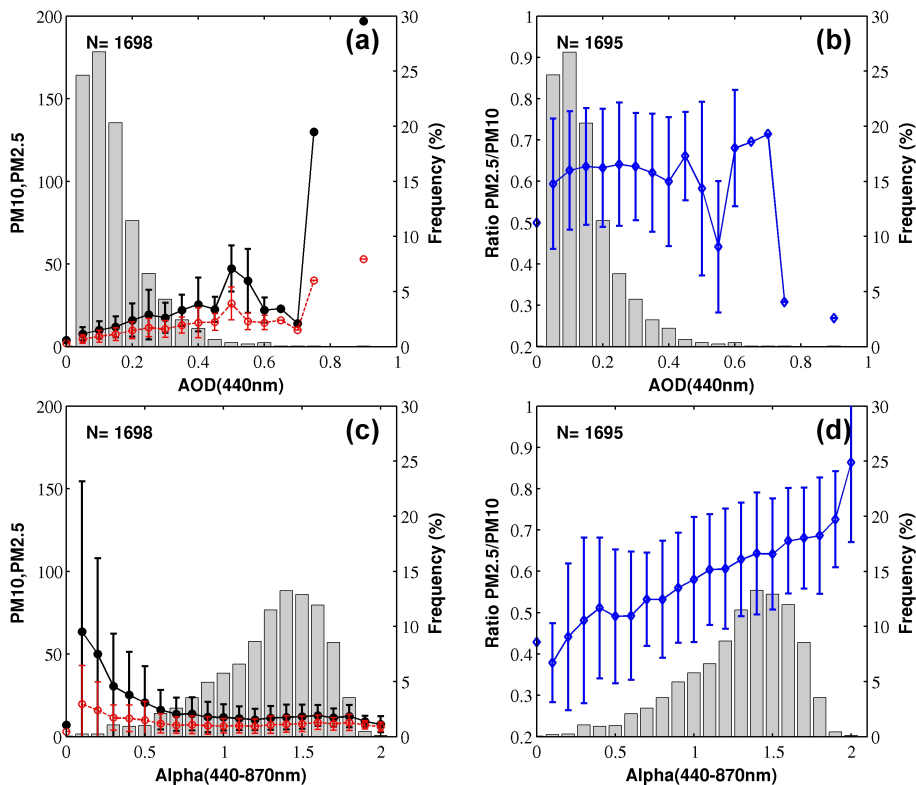


Figure 11. PM₁₀ (curve with filled circles), PM_{2.5} (curve with empty circle) and fine-PM ratio (curve with diamonds) as a function of **(a, b)** binned AOD (440 nm) and **(c, d)** binned Alpha for the period 2003–2011. The bars represent the standard deviation for the EMEP data within each bin. The datacounts for each bin (in percent) are also shown on the superimposed histogram.

Long-term AOD-PM_x relationships in north-nentral Spain

Y. S. Bennouna et al.

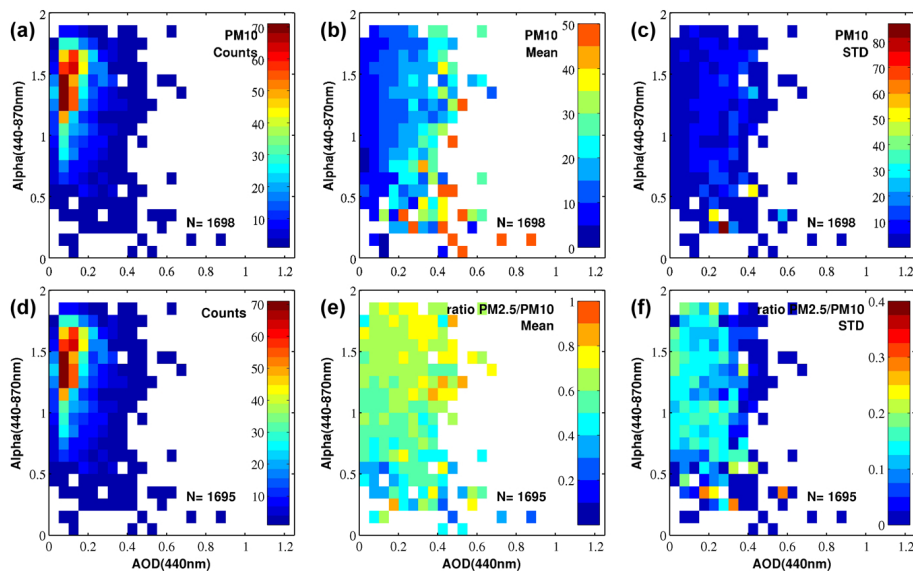


Figure 12. Statistics of PM₁₀ and fine-PM ratio as a function of binned **(a, b)** AOD (440 nm) and **(c, d)** Alpha (440–870 nm) for the period 2003–2011. From left to right, panels correspond to daily data counts, mean and standard deviation.

Title Page

Abstract

Introduction

Conclusions

References

Tables

Figures

◀

▶

◀

▶

Back

Close

Full Screen / Esc

Printer-friendly Version

Interactive Discussion



Long-term AOD-PM_x relationships in north-nentral Spain

Y. S. Bennouna et al.

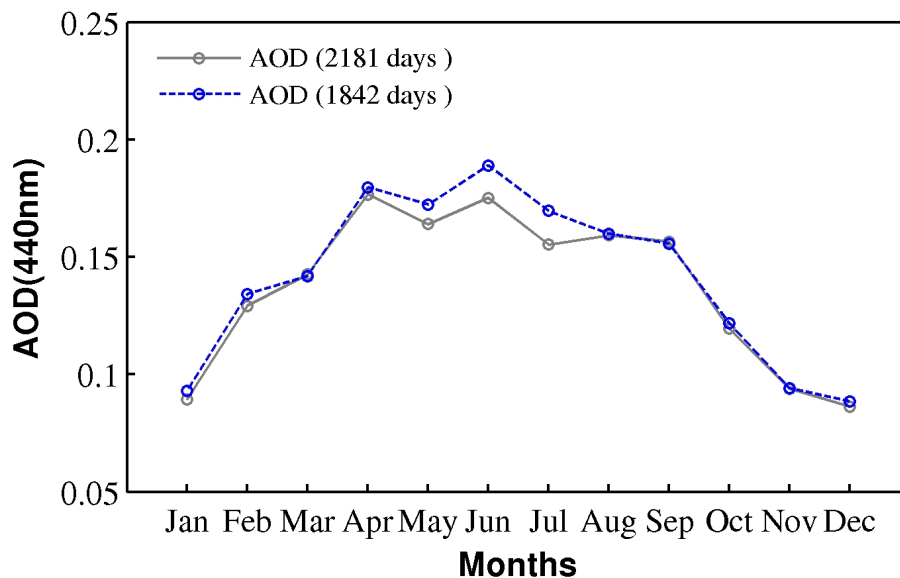


Figure A2. Comparison between the mean annual cycle of the AOD (440 nm) for the period 2003–2011 presented in Fig. 2b (gray curve) with that obtained in Bennouna et al. (2013) (blue curve).

[Title Page](#)[Abstract](#)[Introduction](#)[Conclusions](#)[References](#)[Tables](#)[Figures](#)[◀](#)[▶](#)[◀](#)[▶](#)[Back](#)[Close](#)[Full Screen / Esc](#)[Printer-friendly Version](#)[Interactive Discussion](#)

Long-term AOD-PM_x relationships in north-central Spain

Y. S. Bennouna et al.

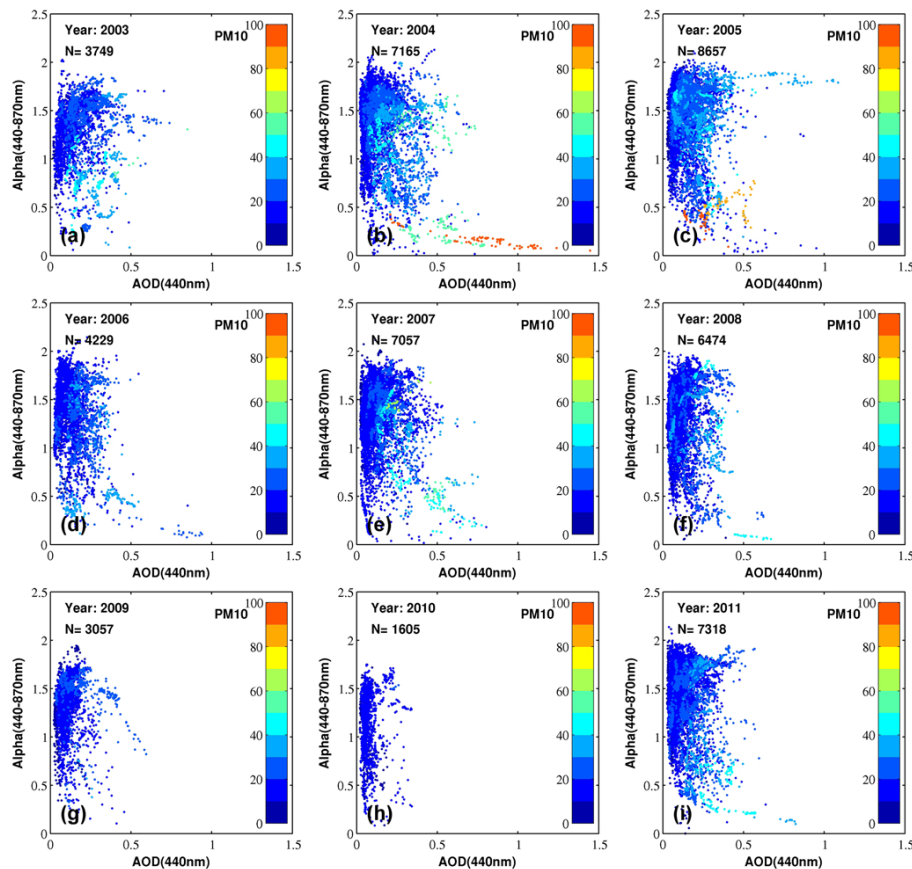


Figure B1. Scatterplots Alpha (440–870 nm) vs. AERONET AOD (440 nm) for instantaneous data (15 min), with corresponding (daily) level of PM₁₀ by year: **(a)** 2003, **(b)** 2004, **(c)** 2005, **(d)** 2006, **(e)** 2007, **(f)** 2008, **(g)** 2009, **(h)** 2010, **(i)** 2011.

Long-term AOD-PM_x relationships in north-nentral Spain

Y. S. Bennouna et al.

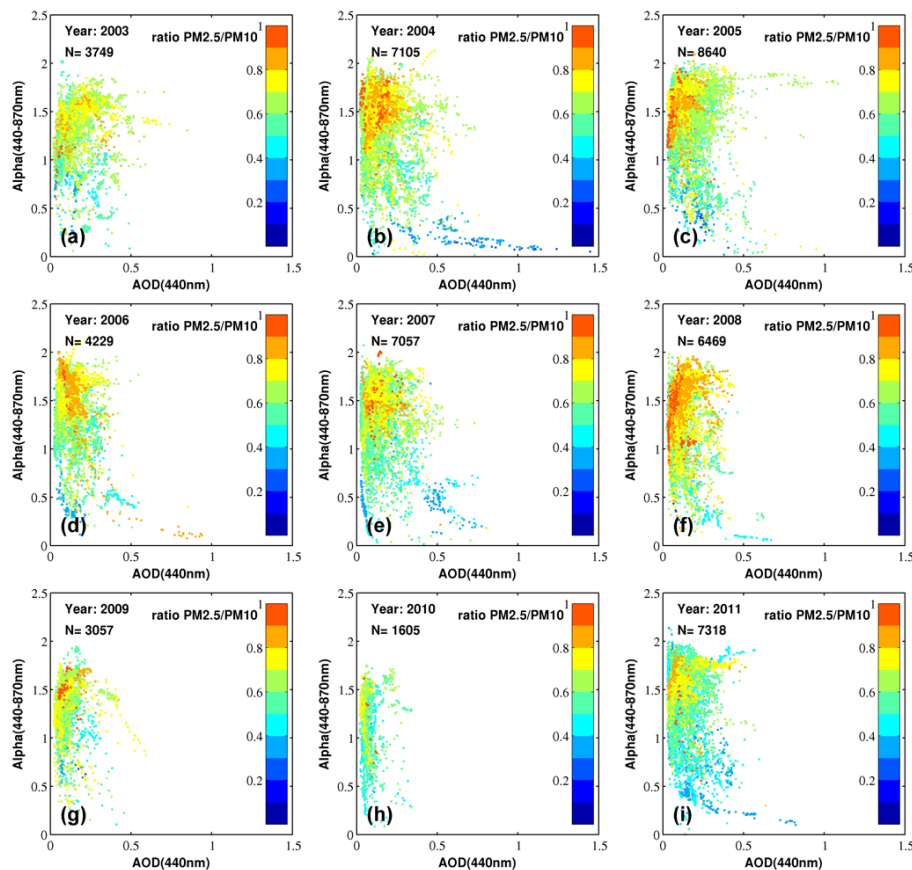


Figure B2. Scatterplots Alpha (440–870 nm) vs. AERONET AOD (440 nm) for instantaneous data (15 min), with corresponding (daily) level of fine/total PM ratio by year: **(a)** 2003, **(b)** 2004, **(c)** 2005, **(d)** 2006, **(e)** 2007, **(f)** 2008, **(g)** 2009, **(h)** 2010, **(i)** 2011.

[Title Page](#)
[Abstract](#)
[Introduction](#)
[Conclusions](#)
[References](#)
[Tables](#)
[Figures](#)

[Back](#)
[Close](#)
[Full Screen / Esc](#)
[Printer-friendly Version](#)
[Interactive Discussion](#)
